Glycobiology, 2015, 1–11
doi: 10.1093/glycob/cwv023
Original Article

OXFORD

Original Article

4-Methylumbelliferone inhibits hepatocellular carcinoma growths by decreasing IL-6 production and angiogenesis

Flavia Piccioni[2], Esteban Fiore[2], Juan Bayo[2], Catalina Atorrasagasti[2,5], Estanislao Peixoto[2], Manglio Rizzo[2], Mariana Malvicini[2,5], Irene Tirado-González[3], Mariana G García[2,5], Laura Alaniz[1,4,5], and Guillermo Mazzolini[1,2,5]

[2]Liver Unit, Gene Therapy Laboratory, Facultad de Ciencias Biomédicas, Universidad Austral, Avenida Presidente Perón 1500 (B1629ODT), Derqui-Pilar, Buenos Aires, Argentina, [3]Laboratory of Reproductive Medicine, Medicine University of Berlin, Charité Centre 12 Internal Medicine and Dermatology, Berlin, Germany, [4]CIT NOBA, Universidad Nacional del Noroeste de la Pcia. de Bs. As., Junín, Buenos Aires, Argentina, and [5]CONICET (Consejo Nacional de Investigaciones Científicas y Técnicas), Buenos Aires, Argentina

[1]To whom correspondence should be addressed: e-mail: gmazzoli@cas.austral.edu.ar (G.D.M.); e-mail: laualaniz@yahoo.com.ar (L.A.)

Received 11 February 2015; Revised 10 April 2015; Accepted 11 April 2015

Abstract

Cirrhosis is characterized by an excessive accumulation of extracellular matrix components including hyaluronic acid (HA) and is widely considered a preneoplastic condition for hepatocellular carcinoma (HCC). 4-Methylumbelliferone (4MU) is an inhibitor of HA synthesis and has anticancer activity in an orthotopic HCC model with underlying fibrosis. Our aim was to explore the effects of HA inhibition by 4MU orally administered on tumor microenvironment. Hepa129 tumor cells were inoculated orthotopically in C3H/HeJ male mice with fibrosis induced by thioacetamide. Mice were orally treated with 4MU. The effects of 4MU on angiogenesis were evaluated by immunostaining of CD31 and quantification of proangiogenic factors (vascular endothelial growth factor, VEGF, interleukin-6, IL-6 and C-X-C motif chemokine 12, CXCL12). IL-6 was also quantified in Hepa129 cells in vitro after treatment with 4MU. Migration of endothelial cells and tube formation were also analyzed. As a result, 4MU treatment decreases tumor growth and increased animal survival. Systemic levels of VEGF were significantly inhibited in 4MU-treated mice. Expression of CD31 was reduced after 4MU therapy in liver parenchyma in comparison with control group. In addition, mRNA expression and protein levels of IL-6 and VEGF were inhibited both in tumor tissue and in nontumoral liver parenchyma. Interestingly, IL-6 production was dramatically reduced in Kupffer cells isolated from 4MU-treated mice, and in Hepa129 cells in vitro. Besides, 4MU was able to inhibit endothelial cell migration and tube formation. In conclusion, 4MU has antitumor activity in vivo and its mechanisms of action involve an inhibition of angiogenesis and IL-6 production. 4MU is an orally available molecule with potential for HCC treatment.

Key words: angiogenesis, HCC, hyaluronic acid, liver fibrosis, IL-6, VEGF, 4-methylumbelliferone

Introduction

Liver fibrosis is a wound-healing process that occurs in response to chronic injuries, mainly chronic hepatitis C and B virus infection, and alcohol abuse (Bataller and Brenner 2005). The chronic insult induces liver injury by production of oxidative stress mediators, cellular DNA damage and necrosis of injured hepatocytes; these alterations are increasingly recognized as a common feature of human hepatocellular carcinoma (HCC; Bataller and Brenner 2005; Hernandez–Gea et al. 2013). Consequently, hepatic stellate cells (HSCs) (Hoshida et al. 2008; Atorrasagasti et al. 2013) and Kupffer cells become activated and secrete extracellular matrix (ECM) components, growth factors and pro-fibrogenic cytokines, promoting migration of endothelial cells, angiogenesis, and fibrosis (Rappaport et al. 1983; Corpechot et al. 2002; Atorrasagasti et al. 2013). Angiogenesis, increased capillarization of sinusoids, and distortion of hepatic vasculature are critically associated with fibrosis progression and hepatocarcinogenesis (Coulon et al. 2011). The liver tumor microenvironment is a complex mixture of cancer cells within the ECM, combined with stromal cells and the proteins they secrete. These components contribute to the hepatocarcinogenic process (Hernandez-Gea et al. 2013). HCC is the most frequent primary liver cancer, and represents the third cause of cancer-related death worldwide (Hernandez–Gea et al. 2013). In addition, HCC is one of the most vascularized solid tumors (Coulon et al. 2011). Neo-angiogenesis is essential for HCC development, progression, and metastasis; cancer cells require oxygen and nutrients for their survival, and they achieve it by induction of a new vascular network (Coulon et al. 2011). Vascular endothelial growth factor (VEGF) is the main proangiogenic factor, which has been reported to increase with HCC progression (Rappaport et al. 1983; Zhu et al. 2011).

HCCs frequently emerge in a diseased liver with an inflammatory microenvironment that finally promotes HCC development. Several inflammatory molecules have been implicated in chronic liver inflammation where a Th2-type cytokine pattern of response is associated with a poor prognosis (Budhu et al. 2006). Prediction of venous metastases, recurrence and prognosis in HCC is based on a unique immune response signature of the liver microenvironment (Budhu et al. 2006). IL-6 is mainly produced by monocytes, macrophages and cancer cells (Nagasaki et al. 2013). Particularly, in cirrhotic livers, IL-6 is highly produced by Kupffer cells and together with other inflammatory mediators has the ability to induce HSCs transdifferentiation to myofibroblasts during fibrogenesis (Bataller and Brenner 2005; Hammerich and Tacke 2014). Moreover, IL-6 is essential for expansion of mutated hepatocytes and subsequent HCC development (He and Karin 2010). Its elevated levels in serum are considered a risk factor of HCC and poor prognosis (Hoshida et al. 2008; Zhu et al. 2011). In addition, IL-6 has been related with tumor progression and angiogenesis in several tumors (He and Karin 2010). Finally, it has been reported that IL-6 binds selectively to hyaluronic acid (HA), dermatan and dextran sulfate, suggesting that this retention and concentration near the site of secretion favors its paracrine and autocrine activity (Vincent et al. 2001).

HA is a large linear glycosaminoglycan (GAG), and is one of the main components of the ECM. It is found in remodeling tissues, since it is implicated in cell proliferation, migration, changes in developing organs, inflammation and tumor progression (Boregowda et al. 2006; Itano et al. 2008). An abnormal production of HA boosts anomalous biologic processes, as observed in several tumors, in which it stimulates invasion and metastasis, and facilitates angiogenesis, among other functions (Toole 2004; Itano et al. 2008). 4-Methylumbelliferone (4MU) is a modified coumarin (7-hydroxy-4-methylcoumarin), widely used orally as choleretic or biliary antispasmodic in humans (Heparvit™) (Takeda and Aburada 1981) as well as in clinical trials in patients with chronic hepatitis B and C (ClinicalTrials.gov identifier: NCT 00225537) (Takeda and Aburada 1981). 4MU inhibits HA-chain elongation by competition, since it is glucuronidated by endogenous UDP-glycosiltransferase. Then, uridine diphosphate glucuronic acid (UDP-GlcUA) molecules, which are substrate of HA synthases, are depleted to form 4MU-GlcUA (Kultti et al. 2009). 4MU also acts by reduction in mRNA levels of HA synthase (Kultti et al. 2009). Its anticancer properties have been demonstrated in several tumor types (Nakazawa et al. 2006; Lokeshwar et al. 2010). It has also been shown that oral 4MU administration has antiangiogenic activity in a cancer murine model (Lokeshwar et al. 2010) and in vitro treatment of endothelial cells (García-Vilas et al. 2013). However, the mechanisms of 4MU modulation in the context of liver fibrosis and HCC have not been reported yet.

In a previous work, we demonstrated that systemic injection of 4MU reduced the degree of liver fibrosis and decreased the number of HCC satellite nodules (Piccioni et al. 2012). In the present work, we elucidate the underlying mechanisms of the antitumor and antifibrotic properties of 4MU orally administered. We explore the effects of HA inhibition in liver tumor microenvironment with a focus on angiogenesis and IL-6 production, since both are key players in liver fibrosis and hepatocarcinogenesis.

Results

4MU treatment impairs HCC growth and increases animal survival

We first studied the antitumoral activity of 4MU administered orally at the dose of 400 mg/kg/day (Figure 1A). The dose was chosen from other studies in which 4MU was orally administered (Yoshihara et al. 2005; Lokeshwar et al. 2010). In a previous work, we observed that intraperitoneal administration of 4MU 20 mg/kg/day significantly reduced the number of tumor satellites with no effects on the main tumor size or animal survival (Piccioni et al. 2012). The present approach resulted in an increased survival rate of 4MU-treated mice from 28.5 to 35.5 days ($P < 0.05$) (Figure 1B). In agreement with this result, the tumor mass–volume was significantly decreased (30 ± 8 vs. 10 ± 3 mm^3; Figure 1C, left panel) as well as the number of satellite nodules, which was 7-fold reduced (2.3 ± 0.6 vs. 0.3 ± 0.2; Figure 1C, right panel). Importantly, serum alanine aminotransferase (ALT) levels were within the normal range in mice after 4MU administration (Figure 1D).

4MU therapy impairs angiogenesis in vivo

It was observed that in both liver fibrosis and HCC the angiogenic process is stimulated (Coulon et al. 2011). It has been demonstrated that HA synthesis is exacerbated in liver fibrosis as well in HCC (Piccioni et al. 2012); therefore, we decided to investigate if there is a link between the therapeutic effects of 4MU and angiogenesis. To this end, microvascular density was first evaluated by immunohistochemistry of platelet endothelial cell adhesion molecule-1 (PECAM-1 or CD31) expression in tumors and liver parenchyma from mice treated with 4MU vs. saline. Although in HCC the CD31 signal was negligible (not shown), in liver parenchyma CD31 positive staining in portal vessels and in fibrotic bridges were observed in saline group (Figure 2A, left panel) and was significantly reduced after treatment with 4MU

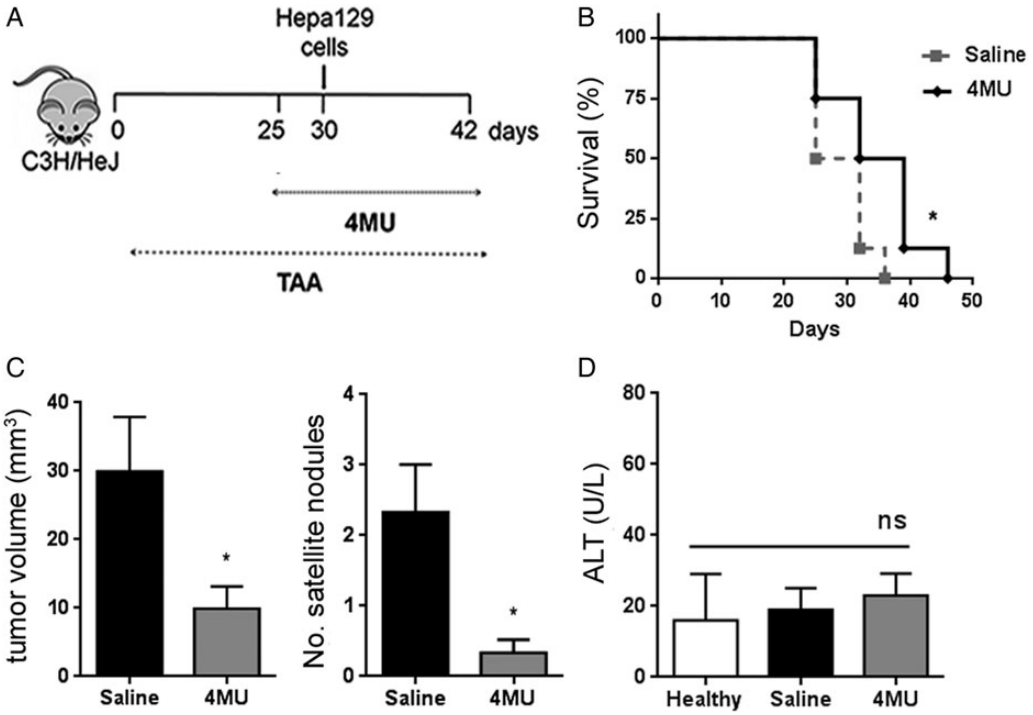

Fig. 1. Antitumor effect of oral 4MU therapy. (**A**) Experimental in vivo model. Fibrosis was induced in C3H/He mice by TAA i.p. injections three times per week for 42 days. At day 30, Hepa129 cells were inoculated into the liver of fibrotic mice. Treatment with 4MU was started 5 days before the surgery, and orally administrated every day, up to animal sacrifice. (**B**) Survival of 4MU-treated mice was analyzed by a Kaplan–Meier curve.*$P < 0.05$ vs. saline, Log-rank test. (**C**) HCC tumor volume was measured with caliper after 12 days from cell inoculation (left panel) and number of satellite nodules were counted (right panel) *$P < 0.05$ vs. saline, Mann–Whitney test. (**D**) ALT serum levels. NS, non significant; Kruskal–Wallis test, ANOVA. Results are representative of at least three independent experiments ($n = 5$–7 per group).

(0.22 ± 0.15 vs. 0.06 ± 0.10% positive area; Figure 2A, right panel). In agreement with this observation, the proangiogenic VEGF immunostaining showed less positive signal in liver parenchyma, fibrotic bridges and portal areas in mice treated with 4MU in comparison with control group (Figure 2B). Tumoral areas exhibited the same tendency, and positive signal was heterogeneously distributed (Figure 2B). We then evaluated VEGF in serum and found that 4MU-treated mice showed a significant reduction in VEGF levels in comparison with non-treated mice (151.3 ± 2.8 vs. 83.8 ± 3.4 pg/mL; Figure 2C).

In order to study the effects of 4MU on tumor angiogenesis, tumor nodules were dissected from the liver parenchyma and changes in proangiogenic molecules were analyzed. Importantly, intratumoral levels of VEGF, detected by ELISA, were significantly reduced when mice were treated with 4MU in comparison with mice treated with saline (1.6 ± 0.6 vs. 0.9 ± 0.2 ng VEGF/total protein; Figure 3A, left panel). Next, we examined by quantitative PCR the expression of C-X-C motif chemokine 12 (CXCL12 or SDF-1) mRNA, a chemokine that is induced downstream of VEGF and has been shown to induce endothelial cell chemotaxis and to stimulate angiogenesis (Grunewald et al. 2006). As a result, the expression of CXCL12 was significantly reduced in tumors from mice treated with 4MU in comparison with mice treated with saline (1.02 ± 0.09 vs. 0.63 ± 0.04; Figure 3A, right panel). In agreement with the results obtained within the HCC, treatment with 4MU reduced the expression of both protein (1.7 ± 0.6 vs. 0.9 ± 0.1 ng VEGF/total protein) and VEGF mRNA (1.06 ± 0.19 vs. 0.47 ± 0.07; Figure 3B) in nontumoral liver parenchyma. In addition, CXCL12 mRNA expression was significantly reduced in 4MU group in nontumoral liver parenchyma (1.02 ± 0.12 vs. 0.53 ± 0.03; Figure 3B, right panel).

4MU modulates IL-6 production in vivo

IL-6 levels, which are generally elevated in HCC (He and Karin 2010), were also reduced in tumor tissue from 4MU-treated mice in comparison with mice treated with saline (188.6 ± 3.7 vs. 88.95 ± 6.2 pg IL-6/mg total protein; Figure 4A). In addition, expression of IL-6 mRNA (1.0 ± 0.2 vs. 0.3 ± 0.1; Figure 4B) and protein (255.40 ± 48.70 vs. 21.14 ± 0.02 pg IL-6/mg total protein; Figure 4B) were significantly reduced in nontumoral liver tissue after 4MU treatment.

HA inhibition by 4MU modulates IL-6 production by HCC and Kupffer cells

In a previous study, we have shown that Hepa129 cells produce large quantities of HA, and that 4MU potently reduced HA production (Piccioni et al. 2012). Given the significant inhibition of IL-6 expression achieved by 4MU therapy, both in HCC tumors and in nontumoral liver parenchyma, we decided to investigate which type of cells were the targets of 4MU. We first treated Hepa129 cells with 4MU for 20 h (in doses that did not induce apoptosis) (Piccioni et al. 2012), and measured IL-6 levels by ELISA. We observed that at 0.25 and 0.5 mM of 4MU, IL-6 levels were notably reduced (1.000 ± 0.045 vs. 0.135 ± 0.078 and 0.010 ± 0.005 pg IL-6/mL, respectively; Figure 4C). However, when we restored the presence of HA, IL-6 production was also restored at 0.25 and 0.5 mM of 4MU (0.508 ± 0.042 and 0.052 ± 0.030 pg IL-6/mL, respectively; Figure 4C, left panel). This result suggests that the decreased production of IL-6 by Hepa129 cells after 4MU therapy is dependent, at least partially, on the inhibition of HA. On the other hand, Kupffer cells are critically involved in fibrogenesis and hepatocarcinogenesis (Naugler et al.

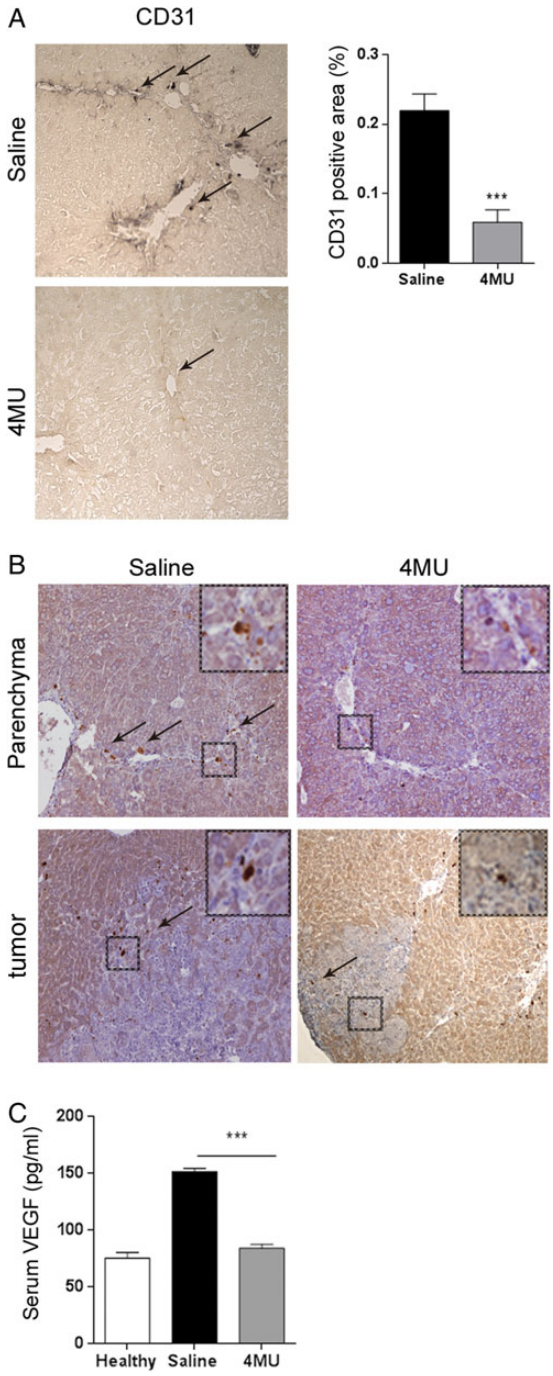

Fig. 2. Angiogenesis is reduced by 4MU therapy. (**A**) Microvascular density in fibrous liver was evaluated by CD31 immunohistochemistry, and quantified by densitometry ***$P < 0.001$ vs. saline, Mann–Whitney test. Arrows indicate positive immunostaining signal. (**B**) Immunostaining for VEGF in liver parenchyma and tumor zone. Positive signal is evidenced as dots around veins or fibrosis bridges (arrows), or heterogeneously distributed in tumor. Magnification 100×. (**C**) Systemic VEGF levels were quantified by ELISA. ***$P < 0.001$ vs. saline, Kruskal–Wallis test, ANOVA. Bars represent the average of measures of each group ± SEM. Results are representative of three independent experiments. This figure is available in black and white in print and in color at *Glycobiology* online.

2007; Hoshida et al. 2008). In order to explore if 4MU has the ability to modify IL-6 production by Kupffer cells in vivo, these cells were isolated from the nontumoral liver parenchyma by a density gradient. We confirmed that these cells were indeed liver macrophages by F4/80 staining (>90% of the cells expressed this marker) (not shown). Importantly, we found a marked reduction of IL-6 protein level produced by Kupffer cells isolated from 4MU-treated mice, in comparison with control group (237.0 ± 19.8 vs. 13.7 ± 1.5 pg IL-6/mg total protein; Figure 4C, right panel).

4MU modulates the angiogenic capability on endothelial cells

Tumor angiogenesis involves a number of events in which the vascular basement membrane of an existing blood vessel is degraded by metalloproteinases, vascular endothelial cells proliferate and migrate, and tube formation is induced by growth factors such as VEGF (Kalluri 2003). We evaluated if vascular endothelial cells (human microvascular endothelial cell, HMEC-1) produce HA and whether 4MU may affect its biosynthesis by an ELISA-like assay. As a result, we observed that HMEC-1 cells produced low levels of HA, which were not influenced by 4MU (Figure 5A, left panel). In addition, HMEC-1 proliferation was not affected by the different doses of 4MU (Figure 5A, right panel). Considering that different factors produced by cancer cells can modulate endothelial cells behavior, we analyzed tube formation capability of HMEC-1 cells incubated with conditioned medium (CM) derived from a line of human HCC cells, Hep3B. For that purpose, HMEC-1 cells were seeded on Matrigel-coated plates and incubated for 6 h with Hep3B CM. Importantly, tube formation was significantly reduced when HMEC-1 cells were incubated with CM obtained from 4MU-pretreated Hep3B cells (0.25 mM 4MU) (88.1 ± 0.9 0 vs. 63.2 ± 5.3 0.25 mM % clear area/field, Figure 5B).

We further evaluated whether HA is able to modulate HMEC-1 cell migration. To this end, HMEC-1 cells or Hep3B cells were pretreated with 4MU for 18 h. In this experiment, CM from Hep3B cells was collected and used as chemoattractant for HMEC-1 cells migration in a Boyden chamber. When we pretreated HMEC-1 cells with 4MU, we observed a significant reduction of their migration capability towards Hep3B CM at the lowest dose of 4MU employed (0.06 mM) (0.82 ± 0.04 0 vs. 0.60 ± 0.06 0.06 mM; Figure 5C). Similar results on HMEC-1 migration were found when they were incubated with CM from 4MU-pretreated Hep3B cells (1.00 ± 0.04 0 vs. 0.57 ± 0.07 0.06 mM; Figure 5D).

Discussion

In this work, we show that oral administration of 4MU in our model of HCC with underlying fibrosis exerts potent antitumor properties in vivo by mechanisms that involved a reduction of proangiogenic factors such as VEGF, CXCL12 and IL-6, both in tumor and in adjacent nontumoral liver parenchyma.

Cancer cells and recruited stromal cells constitute the tumorigenic microenvironment and are the driving force for progression and metastases (Bissell and Radisky 2001). HA is major component of the ECM and is highly expressed in tumor stroma and inflammatory processes (Kojima et al. 1975; Toole 2002, 2004; Boregowda et al. 2006). It has been widely demonstrated that increased production of HA, particularly small HA fragments, is able to induce angiogenesis process in several tumors (West et al. 1985).

We previously demonstrated in our model of HCC and fibrosis that HA inhibition by 4MU reduces liver fibrosis and impairs tumor growth (Piccioni et al. 2012). Increased HA deposition was observed in nontumoral liver parenchyma from mice with fibrosis and in tumor

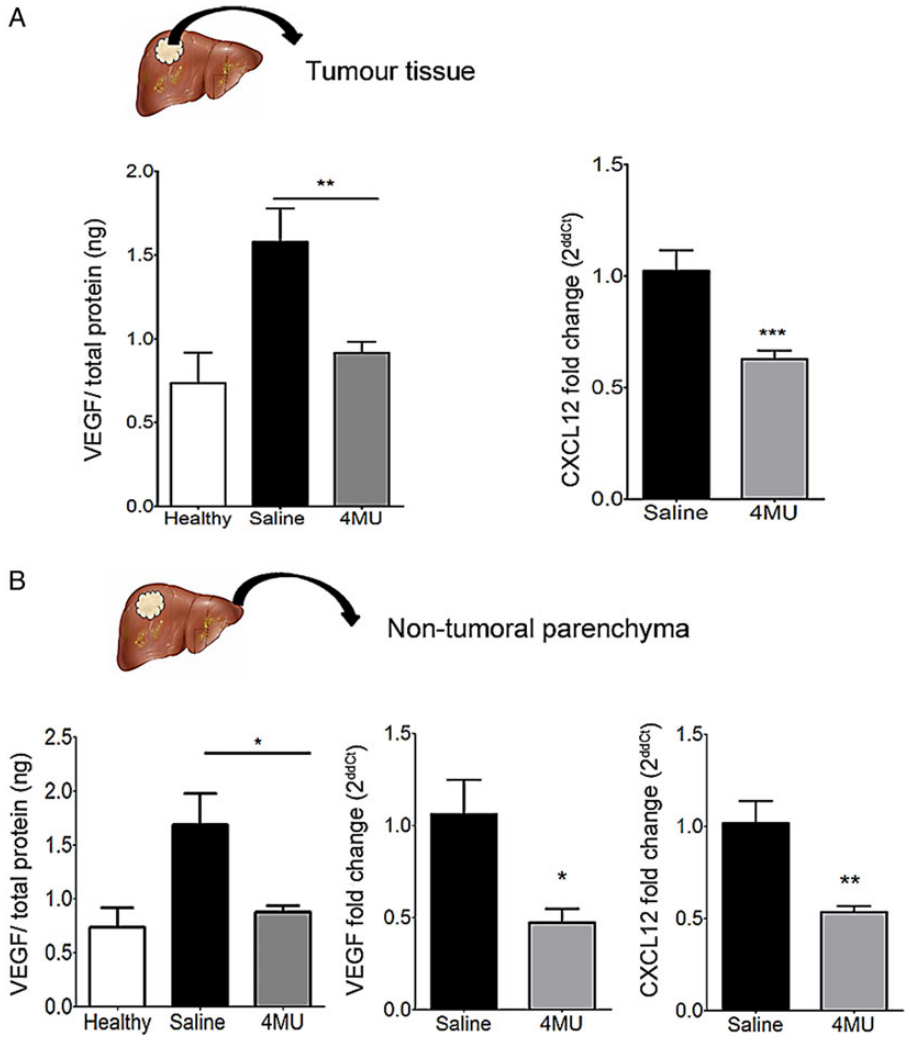

Fig. 3. 4MU reduces the expression of proangiogenic molecules in HCC and its microenvironment. (**A**) Tumor tissue: VEGF was measured from total protein extracts from tumor tissue by ELISA. $^{**}P < 0.01$ vs. saline, Kruskal–Wallis test, ANOVA (left panel). CXCL12 mRNA expression was evaluated by qPCR $^{***}P < 0.001$ vs. saline, Mann–Whitney test (right panel). (**B**) Parenchymal tissue: VEGF protein levels decreased in 4MU-treated mice. $^{*}P < 0.05$ vs. saline, ANOVA. VEGF mRNA (middle panel) and CXCL12 mRNA (right panel) were also reduced, as assessed by qPCR.$^{*}P < 0.05$ and $^{**}P < 0.01$, respectively, vs. saline, Mann–Whitney test. Results are representative of three independent experiments. This figure is available in black and white in print and in color at *Glycobiology* online.

nodules, which were reduced after 4MU therapy (Piccioni et al. 2012). Considering that HA might modulate angiogenesis (Savani et al. 2001), we decided to investigate whether 4MU therapy has an effect on tumor angiogenesis as well as on tumor microenvironment. We hypothesize that inhibition of HA synthesis by 4MU in tumor microenvironment and adjacent nontumoral liver parenchyma, is able to reduce some of the key proangiogenic factors. In our work, oral administration of 4MU significantly prolongs animal survival in comparison with controls. This effect was the result of an important reduction in tumor volume and number of satellite nodules, with no evidence of significant clinical and hepatic, as assessed by liver transaminases, side effects.

Data are scarce regarding the effects of 4MU on tumor angiogenesis. Lokeshwar *et al.* demonstrated that 4MU administration downregulates MMP-2 and -9, and C-X-C motif receptor 4 (CXCR4) in prostate cancer, and observed a reduction of microvascular density (Lokeshwar et al. 2010). Later, García-Vila *et al.* observed antiangiogenic effects of 4MU evaluated in human microvascular endothelial cells and in vivo in chorioallantoic membrane and in a zebrafish model (García-Vilas et al. 2013). Therefore, the effects of 4MU on angiogenesis in the context of HCC and fibrosis have been never studied.

We first investigated if tumor volume reduction was a consequence of angiogenesis modulation by HA-synthesis inhibition achieved with the use of 4MU. For that purpose, we used CD31 immunostaining to evaluate microvessel density in the liver. We found a significant reduction of CD31 positive staining area in the liver parenchyma from 4MU-treated mice in comparison with saline group, although no significant staining was found in the tumor area. Then, the presence of VEGF, the main proangiogenic factor expressed in angiogenesis (Corpechot et al. 2002), was quantified in serum and in tumor and nontumor liver parenchyma. Importantly, we found a significant reduction in VEGF protein level in serum from 4MU-treated mice in comparison with saline group, and the same tendency was observed in liver sections immunostained for VEGF. These results reported here suggest that 4MU has the ability to reduce the pathologic vasculature generated during liver fibrosis. In line with these observations, we separately studied the effects of 4MU on angiogenesis, in HCC tumors and in nontumoral liver parenchyma. We found that in both

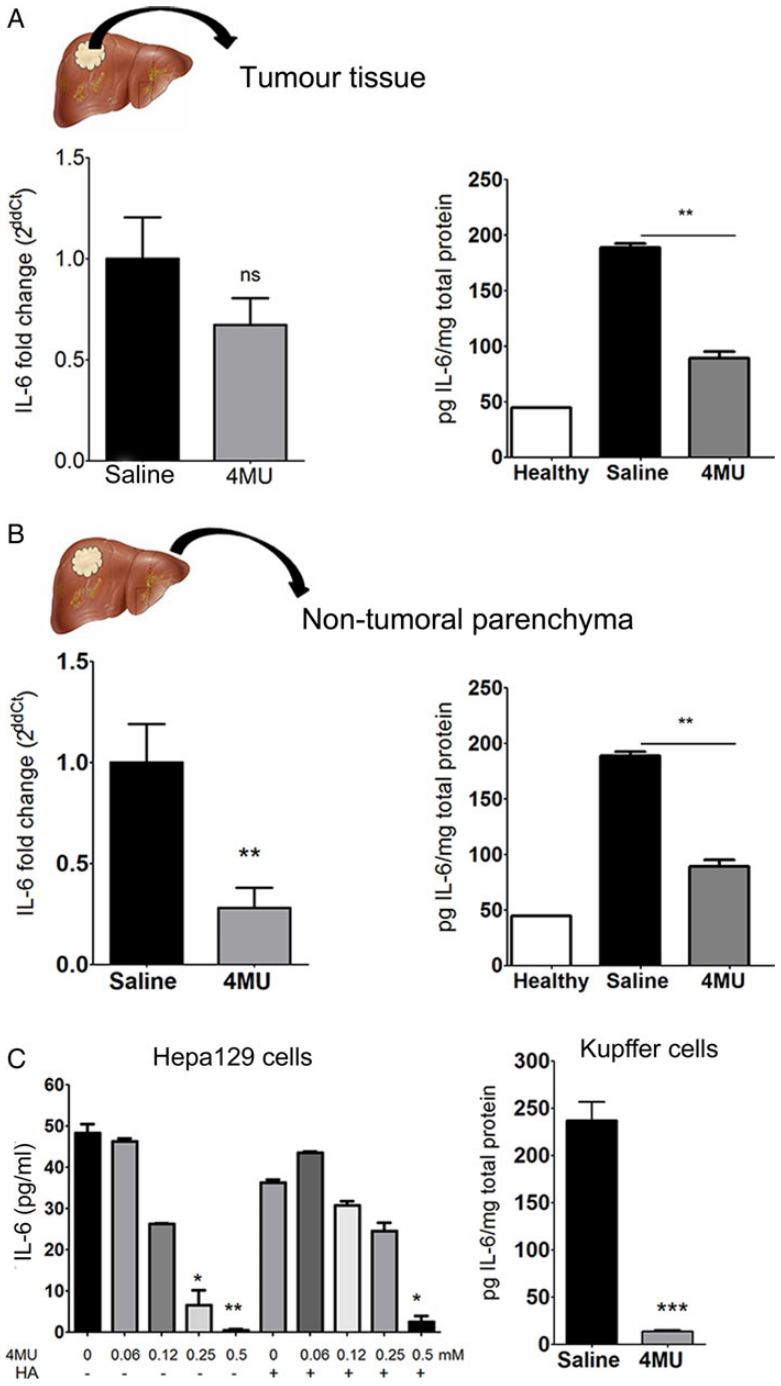

Fig. 4. 4MU modulates IL-6 expression in vivo and in vitro. IL-6 mRNA (left panel) and IL-6 protein (right panel) levels were quantified in tumor tissue (**A**) and parenchymal tissue (**B**) from mice treated with 4MU or saline mice. (A) and (B) right panels: $^{**}P < 0.01$ vs. saline, Kruskal–Wallis test, ANOVA; (A) and (B) left panel: ns, non-significant, $^{**}P < 0.01$ vs. saline, Mann–Whitney test. (**C**) 4MU modulates IL-6 levels in Hepa129 and Kupffer cells. IL-6 protein levels were measured in Hepa129 supernatant, after treatment with 4MU. Incubation with HA recovered IL-6 production at 0.25 mM of 4MU (left panel). $^{*}P < 0.05$ vs. 0 mM, Kruskal–Wallis test, ANOVA. IL-6 produced by Kupffer cells isolated from liver of 4MU-treated or saline group was measured from supernatant (right panel). $^{***}P < 0.001$ vs. saline, Mann–Whitney test. Results are representative of three independent experiments. This figure is available in black and white in print and in color at *Glycobiology* online.

regions there was a significant reduction of VEGF and IL-6 protein expression in 4MU-treated mice when compared with untreated mice. These results are of particular importance since IL-6 is increased in cirrhosis and is a key cytokine for HCC development (He and Karin 2010). Moreover, several IL-6-related angiogenic signaling pathways have been described, such as IL-6/hipoxia-inducible factor-1α in ovary cancer and signal transducer and activator of transcription 3/VEGF in breast cancer (He and Karin 2010). Therefore, IL-6 and VEGF reduction both in liver parenchyma and in tumor suggests an antiangiogenic role for 4MU in our tumor model.

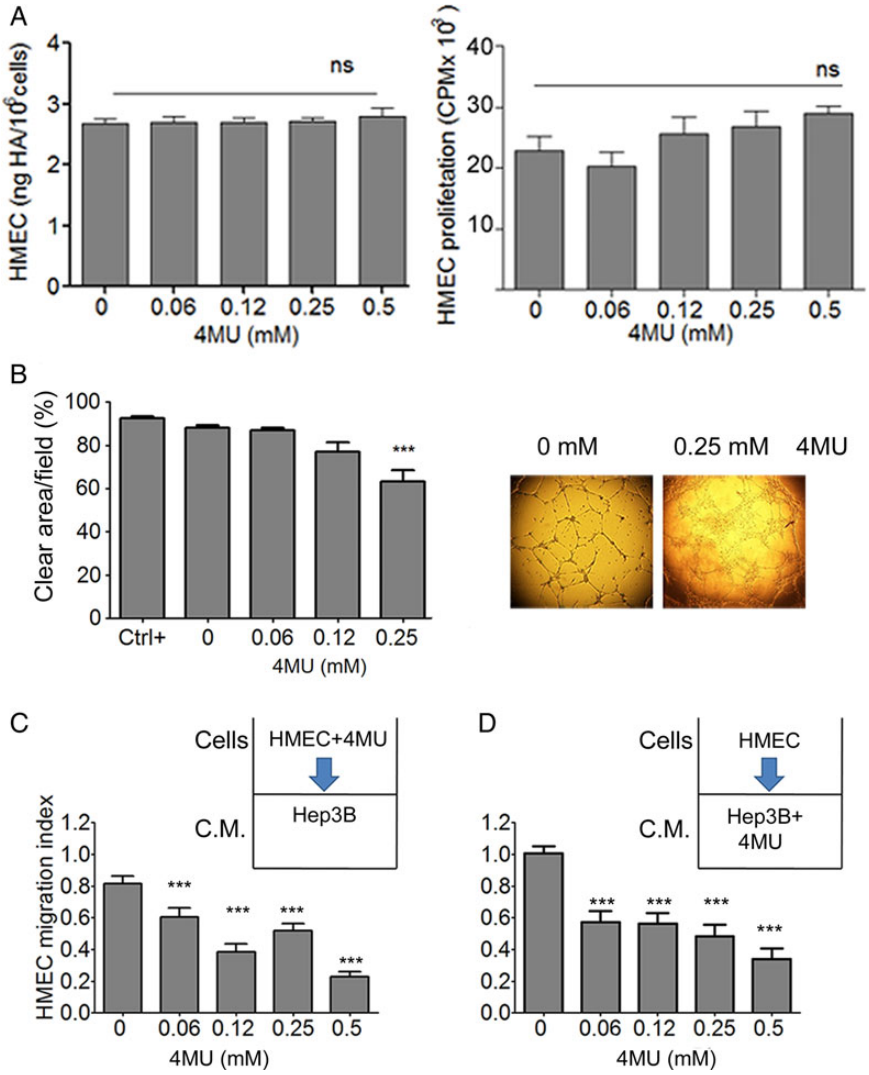

Fig. 5. Inhibition of HA synthesis reduces tube formation and migration of endothelial cells in vitro. (**A**) HA production and proliferation of HMEC cells were not affected by 4MU. (**B**) Tube formation assay was performed stimulating HMEC cells sealed on a Matrigel coat with conditioned medium of Hep3B cells pretreated with different doses of 4MU. Images were taken at 20× and % of clear area/field was quantified. Recombinant VEGF was used to stimulate HMEC-1 cells in the positive control (Ctrl+). ***$P < 0.001$ vs. conditioned medium of Hep3B without pretreatment, Kruskal–Wallis test, ANOVA. (**C**) Migration of HMECs pretreated with 4MU towards Hep3B conditioned medium (CM) and (**D**) HMEC towards conditioned medium of Hep3B pretreated with 4MU were significantly reduced compared with control. ***$P < 0.001$ vs. 0 mM, Kruskal–Wallis test, ANOVA. Results are representative of three independent experiments. This figure is available in black and white in print and in color at *Glycobiology* online.

Grunewald et al. (2006) showed that during injury VEGF induces the expression of CXCL12 (or SDF-1) in perivascular fibroblasts, and concomitantly this chemokine attracts and retains $CXCR4^+$ bone marrow-derived cells, stimulating endothelium vessel proliferation during angiogenesis. In agreement with these observations, CXCL12 mRNA expression was also significantly reduced by 4MU both in tumor and in liver parenchyma, probably related with VEGF downregulation.

In order to dissect which type of cells were responsible for IL-6 modulation by 4MU therapy, we studied IL-6 production by Hepa129 in vitro and by Kupffer cells obtained from the liver parenchyma of mice, using different doses of 4MU. As it was expected, Hepa129 and Kupffer cells produced IL-6, in agreement with several studies that have demonstrated that IL-6 is overproduced in HCC (He and Karin 2010), and Kupffer cells in the context of liver fibrosis (Bataller and Brenner 2005). Importantly, in both type of cells, we found a significant reduction of IL-6 protein levels after 4MU treatment. Interestingly, in Hepa129 tumor cells we observed that the reduction of IL-6 obtained with 0.25 mM of 4MU was reverted by the addition of HA, indicating that the effect was specific of HA inhibition. It has been shown that IL-6 binds selectively to several GAGs, including HA (Ramsden and Rider 1992; Mummery and Rider 2000; Vincent et al. 2001); it was demonstrated in myeloma cells that HA produced could retain and concentrate IL-6 close to the site of secretion favoring an autocrine loop of activation, a feature of this cytokine. Moreover, in a previous work it was shown that HA induces bone marrow macrophages to secrete IL-6 (Noble et al. 1993). Therefore, we might hypothesize that HA overproduced by cancer and stromal cells retain IL-6 secreted by them, favoring an autocrine loop of activation with the outcome of tumor growth stimulation. It has

been observed in injured lungs and fibrosis that HA is accumulated and low-molecular HA fragments stimulate local macrophages to produce inflammatory cytokines and growth factors (Jiang et al. 2011). This, in turn, activates fibroblasts to produce more ECM components. In addition, macrophages express CD44, the main receptor of HA, in their surfaces which indicates that HA binds to these cells (Jiang et al. 2011). These data are in line with the effect of HA-inhibition exerted by 4MU on Kupffer cells in our animal model. However, further studies are needed to dissect the molecular mechanism that leads to the reduction of IL-6 by 4MU in our model.

It is known that factors produced by cancer cells can induce migration of endothelial cells promoting tumor angiogenesis (Carmeliet and Jain 2011). *In vitro* tube formation and migration assays were performed to evaluate 4MU effects on endothelial cells behavior. We observed that 4MU pretreatment of Hep3B cells was able to inhibit tube formation and migration of endothelial cells HMEC-1, when used as a stimulant CM. Although HMEC-1 cells produce low quantities of HA and 4MU does not affect HA synthesis, we found a significant reduction in migration index when they were pretreated with 4MU and migrated towards Hep3B CM. This could possibly occur by some effects of 4MU independent of HA inhibition such as the inhibition of other GAGs. In fact, 4MU acts, at least in part, by depleting UDP-GlcUA, a precursor of other GAGs (Esko et al. 2009). Nevertheless, more studies are needed to explain the mechanism behind the observed effects on endothelial cells.

In conclusion, our study shows that 4MU, an HA-synthesis inhibitor, has antitumor activity in vivo and its mechanisms of action involve a reduction of the proangiogenic factors VEGF and CXCL12, as well as a decrease of IL-6 production in liver tumor microenvironment; therefore, 4MU is a promising therapeutic molecule for HCC.

Materials and methods

Cell lines

Mouse HCC cells syngeneic with C3H/HeJ mice (Hepa129) were kindly provided by Dr. Volker Schmitz (Bonn University, Germany). A cell line of human hepatocelullar carcinoma (Hep3B) was purchased by ATCC, Manassas, VA. Human microvascular endothelial cells (HMEC-1) were from CDC (Centers for Disease Control, Atlanta, GA). Cell lines were cultured in complete DMEM (2 mM glutamine, 100 U/mL penicillin and 100 mg/mL streptomycin) and 10% heat-inactivated fetal bovine serum (FBS), except for Hepa129 cells that were grown in RPMI 1640 (GIBCO, Invitrogen Argentina) and supplemented with 10% FBS and 55 µM 2-mercaptoethanol (GIBCO).

Conditioned medium

To obtain cell CM, Hep3B cells were cultured as previously described to 90% confluence and then washed with PBS and cultured with complete DMEM without FBS. Eighteen hours later, CM was harvested and stored at −80°C until use.

Mice and in vivo experiments

Six-to-eight-week-old male C3H/HeJ mice were purchased from Comisión Nacional de Energía Atómica, Ezeiza, Buenos Aires, Argentina. Animal care and experimental procedures were followed according to institutional guidelines and conformed to requirement of the state authority for animal research conduct. Fibrosis was induced by intraperitoneal (i.p.) injections of thioacetamide (TAA) (at a dose of 200 mg/kg; Sigma-Aldrich, St. Louis) thrice weekly for 42 days. On day 30, orthotopic tumors were established by subcapsular inoculation of 1.25×10^5 Hepa129 cells into the left liver lobe by laparotomy (Piccioni et al. 2012). Five days before tumor implantation, a group of mice received 4MU (Sigma-Aldrich) treatment by oral gavage at a dose of 400 mg/kg/day, for 20 days (4MU group). Twelve days after tumor implantation, mice were sacrificed (Figure 1A). For serum sampling, blood from retro-orbital bleeding was collected in heparin-free tubes. Tumor volume (mm^3) was calculated by the formula $\pi/6 \times$ larger diameter $\times$ (smaller diameter)^2, by caliper measurement. Number of HCC satellites were also quantified. For pathology studies, sections of liver including the tumor were taken and fixed in formalin 10% until paraffin inclusion. For quantitative PCR and ELISA from tissue homogenates, tumors were separated from liver parenchyma by a clear cut with a scalpel.

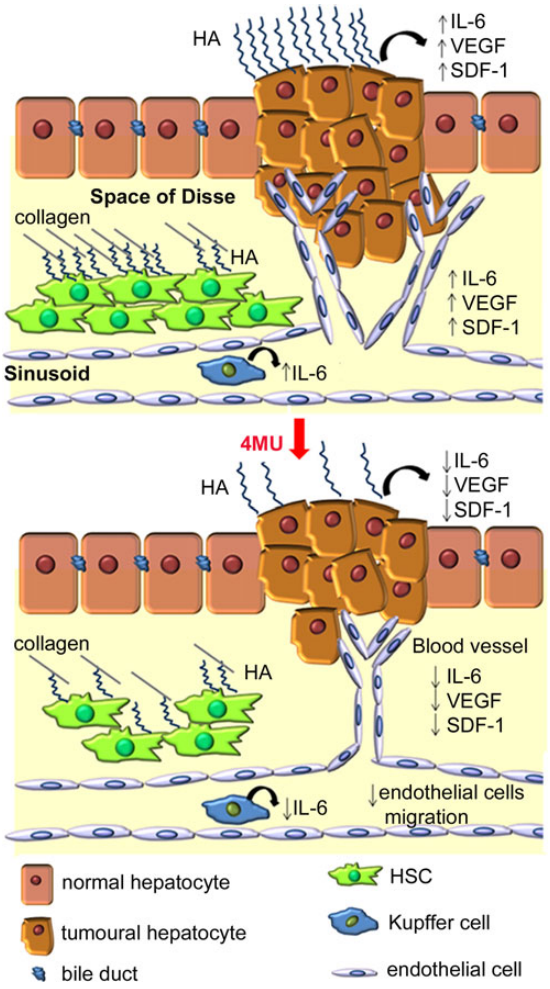

Fig. 6. A model for the proposed mechanism of action of 4MU on HCC with underlying fibrosis. 4MU modulates liver fibrosis by inhibition of HSC proliferation, and its collagen and HA production (Piccioni *et al.*). 4MU also reduces HA produced by HCC, and inhibits its growth by reducing the proangiogenic factors VEGF and CXCL12 both in tumor and nontumoral liver parenchyma. The pro-inflammatory cytokine IL-6, a key cytokine in HCC progression, is also inhibited by 4MU treatment. In addition, IL-6 production by Kupffer cells is also decreased by 4MU. Finally, liver endothelial cells were reduced in liver parenchyma by 4MU therapy; migration and tube formation by endothelial cells were also inhibited in vitro suggesting an antiangiogenic effect of 4MU.

Liver transaminases

Serum ALT levels were measured using an ARCHITECT® (Abbott, Buenos Aires, Argentina) autoanalyzer.

CD31 immunostaining

Briefly, paraffin liver sections of 5 μm thick were rehydrated. Antigen retrieval was performed by incubation with 20 μg/mL Proteinase K for 20 min at room temperature (RT). After washing with tap water, slides were incubated with 3% H_2O_2 in distilled water for 30 min at RT to block endogenous peroxidase, followed by avidin and biotin and blocking (Vector Laboratories, Inc. Burlingame, CA). Protein was blocked with 2.5% BSA/PBS/Tween0.1% solution for 10 min at RT. Sections were then incubated with a rat antibody to CD31 (Abcam, MA) 1 : 100 in PBS overnight at 4°C, and then with a biotinylated anti-rabbit secondary antibody (Vector Laboratories, Inc.) 1 : 100 in 0.2% BSA in PBS at RT for 1 h. Peroxidase complex (Sigma-Aldrich) 1 : 10 in PBS was used as a revealing system. The signal was detected by 0.1% diaminobenzidine (Sigma-Aldrich), 4% glucose, 0.08% $ClNH_4$, 5% nickel ammonium sulfate in 0.2 M AcNa and 0.05% H_2O_2. Densitometric analysis was performed by taking 10 images/slide at 400× (Nikon Eclipse E800, Nikon, Buenos Aires, Argentina) and percentage of positive area was calculated with ImageJ software (National Institutes of Health, Bethesda, MD).

Enzyme-linked immunosorbent assay

Serum samples, liver homogenates or conditioned media were tested in competitive ELISA using kits obtained from R&D Systems to quantify VEGF, following the manufacturer's recommendations. IL-6 levels were determined using BD OptEIA™ Set Mouse IL-6 (BD Bioscience, CA) following the manufacturer's recommendations.

VEGF immunostaining

Briefly, 8 μm thick cryosections were fixed in acetone for 10 min. After washes in PBS, sections were dehydrated in increasing alcohol passages until xylene, and rehydrated in reverse order. Endogenous peroxidase was blocked with 3% H_2O_2 in methanol for 30 min at RT. Then, endogenous avidin and biotin were blocked using Blocking Kit (Vector Laboratories, Inc.). Afterwards, proteins were blocked by incubation with 1% BSA/PBS. Primary antibody anti-VEGF (sc-147, Santa Cruz Biotechnology) 1 : 100 in 1% BSA/PBS/0.1% Triton was incubated for 18 h at 4°C. The negative control was performed without primary antibody. After washes in PBS, biotinylated anti-rabbit secondary antibody 1 : 400 was incubated for 2 h at RT. Revealing system was the same as for CD31 immunostaining. The counterstaining was performed incubating for 10 s with haematoxylin solution (Biopur, Bs.As, Argentina).

Reverse transcription-polymerase chain reaction

Total RNA from tumor, liver tissue or cells were extracted using Trizol Reagent (Sigma-Aldrich). Total RNA (2 μg) was reverse transcribed with 200 U of SuperScript II Reverse Transcriptase (Invitrogen, Carlsbad, CA) using 500 ng of Oligo primers. cDNAs were subjected to real-time polymerase chain reaction (qPCR) (Stratagene Mx3005p, Stratagene, CA). For qRT-PCR, the mRNA levels of VEGF, IL-6 and CXCL12 were quantified by SYBR®Green (Invitrogen, Bs. As, Argentina), using the following primers: VEGF forward 5′-GTGCACTGGACCCTGGCTTTA-3′ and reverse 5′-GGTCTCAATCGGACGGCAGTA-3′; IL-6 forward 5′-AGTTGCCTTCTTGGGACTGA-3′ and reverse 5′-TCCACGATTTCCCAGAGAAC-3′; CXCL12 forward 5′-GAGAGCCACATCGCCAGAG-3′ and reverse 5′-TTTCGGGTCAATGCACACTTG-3′. PCR amplifications were carried out using a cycle of 95°C for 10 min and 40 cycles under the following parameters: 95°C for 30, 56°C for 30 s, 72°C for 1 min. At the end of PCR reaction, the temperature was increased from 60 to 95°C at a rate of 2°C/min, and the fluorescence was measured every 15 s to construct the melting curve. Values were normalized to levels of glyceraldehyde-3-phosphate dehydrogenase (used as housekeeping) transcript (forward 5′-CATCTCTGCCCCCTCTGCTG-3′ and reverse 5′-GCCTGCTTCACCACCTTCTTG-3′). Data were processed by the ΔΔCt method (Atorrasagasti et al. 2013). The relative amount of the PCR product amplified from untreated cells was set as 1. A nontemplate control was run in every assay, and all determinations were performed as triplicates in three separated experiments.

IL-6 quantification

Hepa129 cells (5×10^6 cells/well) were incubated with 4MU (0, 0.06, 0.12, 0.25 and 0.5 mM) for 20 h. After washing, they were subsequently incubated with high-molecular-weight (HMW) HA 200 μg/μL for other 20 h. Finally, supernatant was subjected to IL-6 quantification by ELISA. Recombinant HMW-HA (native HA) 1.5–1.8×10^6 Da (CPN spol.s.r.o, Czech Republic) was kindly donated by Farmatrade, Argentina.

Kupffer cells isolation

Primary culture of murine Kupffer cells from mice treated with 4MU or control group (saline) was obtained through liver perfusion with collagenase (Sigma-Aldrich) and subsequent washes and separation by a density gradient with Histodenz (Sigma-Aldrich) 30% in PBS, as described elsewhere (Hansen et al. 2002). After 10 min of incubation in a 24-well plate of the cell suspension obtained, Kupffer cells remained adhered to plastic. Then, they were maintained in RPMI medium supplemented with 10% FBS for 24 h, and supernatants were collected for IL-6 quantification. Cells were immunostained with a rat antimouse F4/80 antibody (Abcam) 1 : 350 in PBS for 45 min at 4°C. After three washes with 1%BSA/PBS, cells were incubated with a fluorescein isothiocyanate antirat (Vector Laboratories, Inc.) antibody 1 : 100 in PBS for 45 min at 4°C. Then, cells were observed under a fluorescence microscope (Nikon Eclipse E800, Nikon, Buenos Aires, Argentina).

HA quantification by an ELISA-like assay

HA from cell-free supernatants were measured using a competitive ELISA-like assay as described elsewhere (Cordo-Russo et al. 2009). Briefly, 96-well microplates (Nunc, Thermo Fisher Scientific Inc., MA) were coated with 100 μg/mL of HA (CPN spol.s.r.o. Czech Republic). Then, wells were incubated with 25 μL of sample or standard HA (0–1) and 0.75 μg/mL of biotinylated HA-binding protein (bHA-BP; Calbiochem, MA) at 37°C for 4 h, and next washed with PBS/0.05% Tween-20. The bHA-BP bound to the wells was determined using an avidin–biotin detection system (Sigma-Aldrich). Sample concentrations were calculated from a standard curve generated by plotting the absorbance at 490 nm against the concentration of HA (Cordo-Russo et al. 2009). Cell-free culture supernatants were obtained from 1×10^6 HMEC-1 cells incubated with 4MU for 24 h.

Cell proliferation assay

For the proliferation assay, HMEC-1 cells (2.5×10^5/well) were incubated in a 24-well plate with 4MU at different concentrations (0, 0.06, 0.12, 0.25 and 0.5 mM). After 48 h, cultures were pulsed

with 5 μCi/mL [methyl 3H] thymidine for the last 6 h. Then, cells were lysed and the incorporation of radioactivity was measured in a liquid scintillation β-counter (Beckman Coulter, CA).

Tube formation assay

Tube formation assay was performed using Matrigel (BD Bioscience), thawed at 4°C to prevent polymerization. Forty microliters of Matrigel/well were seeded in a 96-well culture plate (GBO, Frickenhausen), and allowed to polymerize at 37°C for at least 30 min. HMEC-1 cells (2×10^4), FBS strarved 18 h before, were seeded in 90 μL of FBS-free DMEM, and stimulated with 10 μL of 4MU-pretreated Hep3B conditioned media. For positive control, 100 ng/mL of human recombinant VEGF (Calbiochem) was used to stimulate HMEC-1 cells. After 6 h of incubation at 37°C, cells were stained and fixed with Crystal Violet solution. Quantification was performed by analyzing the cell-free area from three images per well at 100× (Nikon, Buenos Aires, Argentina) with Image J software (National Institutes of Health, Bethesda, MD).

In vitro migration assay

In vitro migration was performed using a 48-Transwell microchemotaxis Boyden Chamber unit (Neuroprobe, Inc.). HMEC-1 (1.5×10^3 cells/well) were placed in the upper chamber and DMEM or Hep3B CM were applied to the lower chamber of the transwell unit. Chemokinesis controls were performed placing Hep3B CM in the upper and lower chamber. The system was left for 4 h at 37°C in a 5% CO_2 humidified atmosphere. Cells attached to the lower side of the membrane were fixed in 2% formaldehyde, stained with 4′,6-diamidino-2-phenylindole dihydrochloride (Sigma-Aldrich) and counted using fluorescent-field microscopy at 100×. Captured images from three representative visual fields were analyzed using CellProfiler software (www.cellprofiler.com), and the mean number of cells/field ± SEM was calculated.

Ethics statement

Animals were maintained at our Animal Resource Facilities (Facultad de Ciencias Biomédicas, Universidad Austral) in accordance with the experimental ethical committee and the NIH guidelines on the ethical use of animals. The "Animal Care Committee" from Facultad de Ciencias Biomédicas, Universidad Austral, approved the experimental protocol.

Statistical analysis

All experiments were performed in triplicate and repeated at least three times on different occasions. Values were expressed as the mean ± SEM. The Mann–Whitney or Kruskal–Wallis (ANOVA) tests were used to evaluate the statistical differences between two or more than two groups, respectively. Mice survival was analyzed by a Kaplan–Meier curve. A P-value of <0.05 was considered as significant. Prism software (Graph Pad, San Diego, CA) was employed for the statistical analysis.

Funding

This work was supported by grants from Austral University (to M.R.: I01-12; F.P.: I02-12; M.G.: T13-12) and from Agencia Nacional de Promoción Científica y Tecnológica (ANPCyT) grants (L.A.: PICT-2007/00082; M.G.: PICTO 2008/00115; M.G. and G.M.: PICT 2010/2818; G.M. and L.A.: PICT 2012/1407).

Acknowledgements

We thank Flavia V. Ferreira and Guillermo A. Gastón for their expert technical assistance.

Conflict of interest

None declared.

Abbreviations

4MU, 4-methylumbelliferone; bHA-BP, biotinylated HA-binding protein; CM, conditioned medium; CXCL12, C-X-C motif chemokine 12; CXCR4, C-X-C motif receptor 4; ECM, extracellular matrix; GAG, glycosaminoglycan; HA, hyaluronic acid;; HCC, hepatocellular carcinoma; HMW, high-molecular weight; HSC, hepatic stellate cell; IL-6, interleukin-6; TAA, thioacetamide; UDP-GlcA, uridine diphosphate glucuronic acid; VEGF, vascular endothelial growth factor.

References

Atorrasagasti C, Peixoto E, Aquino JB, Kippes N, Malvicini M, Alaniz L, Garcia M, Piccioni F, Fiore EJ, Bayo J. 2013. Lack of the matricellular protein SPARC (secreted protein, acidic and rich in cysteine) attenuates liver fibrogenesis in mice. *PLoS ONE*. 8(2):e54962.

Bataller R, Brenner DA. 2005. Liver fibrosis. *J Clin Invest*. 115(2):209–218.

Bissell MJ, Radisky D. 2001. Putting tumours in context. *Nat Rev Cancer*. 1 (1):46–54.

Boregowda RK, Appaiah HN, Siddaiah M, Kumarswamy SB, Sunila S, Thimmaiah K, Mortha K, Toole B, Banerjee Sd. 2006. Expression of hyaluronan in human tumor progression. *J Carcinog*. 5(1):2.

Budhu A, Forgues M, Ye QH, Jia HL, He P, Zanetti KA, Kammula US, Chen Y, Qin LX, Tang ZY. 2006. Prediction of venous metastases, recurrence, and prognosis in hepatocellular carcinoma based on a unique immune response signature of the liver microenvironment. *Cancer Cell*. 10(2):99–111.

Carmeliet P, Jain RK. 2011. Molecular mechanisms and clinical applications of angiogenesis. *Nature*. 473(7347):298–307.

Cordo-Russo R, Garcia M, Barrientos G, Orsal A, Viola M, Moschansky P, Ringel F, Passi L, Alaniz L, Hajos S. 2009. Murine abortion is associated with enhanced hyaluronan expression and abnormal localization at the fetomaternal interface. *Placenta*. 30(1):88–95.

Corpechot C, Barbu V, Wendum D, Kinnman N, Rey C, Poupon R, Housset C, Rosmorduc O. 2002. Hypoxia-induced VEGF and collagen I expressions are associated with angiogenesis and fibrogenesis in experimental cirrhosis. *Hepatology*. 35(5):1010–1021.

Coulon S, Heindryckx F, Geerts A, Van Steenkiste C, Colle I, Van Vlierberghe H. 2011. Angiogenesis in chronic liver disease and its complications. *Liver Int*. 31(2):146–162.

Esko JD, Kimata K, Lindahl U. 2009. Proteoglycans and sulfated glycosaminoglycans. 2nd ed. New York (NY): Cold Spring Harbor Laboratory Press.

García-Vilas JA, Quesada AR, Medina MAn. 2013. 4-Methylumbelliferone inhibits angiogenesis in vitro and in vivo. *J Agric Food Chem*. 61 (17):4063–4071.

Grunewald M, Avraham I, Dor Y, Bachar-Lustig E, Itin A, Yung S, Chimenti S, Landsman L, Abramovitch R, Keshet E. 2006. VEGF-induced adult neovascularization: Recruitment, retention, and role of accessory cells. *Cell*. 124 (1):175–189.

Hammerich L, Tacke F. 2014. Interleukins in chronic liver disease: Lessons learned from experimental mouse models. *Clin Exp Gastroenterol*. 7:297.

He G, Karin M. 2010. NF-κB and STAT3 – key players in liver inflammation and cancer. *Cell Res*. 21(1):159–168.

Hernandez–Gea V, Toffanin S, Friedman SL, Llovet JM. 2013. Role of the microenvironment in the pathogenesis and treatment of hepatocellular carcinoma. *Gastroenterology*. 144(3):512–527.

Hoshida Y, Villanueva A, Kobayashi M, Peix J, Chiang DY, Camargo A, Gupta S, Moore J, Wrobel MJ, Lerner J. 2008. Gene expression in fixed

tissues and outcome in hepatocellular carcinoma. *New Engl J Med*. 359 (19):1995–2004.

Itano N, Zhuo L, Kimata K. 2008. Impact of the hyaluronan-rich tumor microenvironment on cancer initiation and progression. *Cancer Sci*. 99(9): 1720–1725.

Jiang D, Liang J, Noble PW. 2011. Hyaluronan as an immune regulator in human diseases. *Physiol Rev*. 91(1):221–264.

Kalluri R. 2003. Basement membranes: Structure, assembly and role in tumour angiogenesis. *Nat Rev Cancer*. 3(6):422–433.

Kojima J, Nakamura N, Kanatani M, Omori K. 1975. The glycosaminoglycans in human hepatic cancer. *Cancer Res*. 35(3):542–547.

Kultti A, Pasonen-Seppänen S, Jauhiainen M, Rilla KJ, Kärnä R, Pyöriä E, Tammi RH, Tammi MI. 2009. 4-Methylumbelliferone inhibits hyaluronan synthesis by depletion of cellular UDP-glucuronic acid and downregulation of hyaluronan synthase 2 and 3. *Exp Cell Res*. 315(11):1914–1923.

Lokeshwar VB, Lopez LE, Munoz D, Chi A, Shirodkar SP, Lokeshwar SD, Escudero DO, Dhir N, Altman N. 2010. Antitumor activity of hyaluronic acid synthesis inhibitor 4-methylumbelliferone in prostate cancer cells. *Cancer Res*. 70(7):2613–2623.

Mummery RS, Rider CC. 2000. Characterization of the heparin-binding properties of IL-6. *J Immunol*. 165(10):5671–5679.

Nagasaki T, Hara M, Nakanishi H, Takahashi H, Sato M, Takeyama H. 2013. Interleukin-6 released by colon cancer-associated fibroblasts is critical for tumour angiogenesis: Anti-interleukin-6 receptor antibody suppressed angiogenesis and inhibited tumour–stroma interaction. *Br J Cancer*. 110 (2):469–478.

Nakazawa H, Yoshihara S, Kudo D, Morohashi H, Kakizaki I, Kon A, Takagaki K, Sasaki M. 2006. 4-methylumbelliferone, a hyaluronan synthase suppressor, enhances the anticancer activity of gemcitabine in human pancreatic cancer cells. *Cancer Chemother Pharmacol*. 57(2):165–170.

Naugler WE, Sakurai T, Kim S, Maeda S, Kim K, Elsharkawy AM, Karin M. 2007. Gender disparity in liver cancer due to sex differences in MyD88-dependent IL-6 production. *Science*. 317(5834):121–124.

Noble PW, Lake F, Henson P, Riches D. 1993. Hyaluronate activation of CD44 induces insulin-like growth factor-1 expression by a tumor necrosis factor-alpha-dependent mechanism in murine macrophages. *J Clin Invest*. 91(6):2368.

Piccioni F, Malvicini M, Garcia MG, Rodriguez A, Atorrasagasti C, Kippes N, Buena ITP, Rizzo MM, Bayo J, Aquino J. 2012. Antitumor effects of hyaluronic acid inhibitor 4-methylumbelliferone in an orthotopic hepatocellular carcinoma model in mice. *Glycobiology*. 22(3):400–410.

Ramsden L, Rider CC. 1992. Selective and differential binding of interleukin (IL)-1α, IL-1β, IL-2 and IL-6 to glycosaminoglycans. *Eur J Immunol*. 22 (11):3027–3031.

Rappaport A, MacPhee P, Fisher M, Phillips M. 1983. The scarring of the liver acini (cirrhosis). *Virchows Archiv A*. 402(2):107–137.

Savani RC, Cao G, Pooler PM, Zaman A, Zhou Z, DeLisser HM. 2001. Differential involvement of the hyaluronan (HA) receptors CD44 and receptor for HA-mediated motility in endothelial cell function and angiogenesis. *J Biol Chem*. 276(39):36770–36778.

Hansen B, Arteta B, Smedsrød B. 2002. The physiological scavenger receptor function of hepatic sinusoidal endothelial and Kupffer cells is independent of scavenger receptor class A type I and II. *Mol Cell Biochem*. 240: 1–8.

Takeda S, Aburada M. 1981. The choleretic mechanism of coumarin compounds and phenolic compounds. *J Pharmacobio-Dyn*. 4(9):724–734.

Toole BP. 2004. Hyaluronan: From extracellular glue to pericellular cue. *Nat Rev Cancer*. 4(7):528–539.

Toole BP. 2002. Hyaluronan promotes the malignant phenotype. *Glycobiology*. 12(3):37R–42R.

Vincent T, Jourdan M, Sy M-S, Klein B, Mechti N. 2001. Hyaluronic acid induces survival and proliferation of human myeloma cells through an interleukin-6-mediated pathway involving the phosphorylation of retinoblastoma protein. *J Biol Chem*. 276(18):14728–14736.

West DC, Hampson IN, Arnold F, Kumar S. 1985. Angiogenesis induced by degradation products of hyaluronic acid. *Science*. 228(4705):1324–1326.

Yoshihara S, Kon A, Kudo D, Nakazawa H, Kakizaki I, Sasaki M, Endo M, Takagaki K. 2005. A hyaluronan synthase suppressor, 4-methylumbelliferone, inhibits liver metastasis of melanoma cells. *FEBS Lett*. 579(12):2722–2726.

Zhu AX, Duda DG, Sahani DV, Jain RK. 2011. HCC and angiogenesis: Possible targets and future directions. *Nat Rev Clin Oncol*. 8(5):292–301.